

## Feedback suppression of rotating external kink instabilities in the presence of noise

Jeremy M. Hanson,<sup>a)</sup> Bryan De Bono, Royce W. James, Jeffrey P. Levesque, Michael E. Mauel, David A. Maurer, Gerald A. Navratil, Thomas Sunn Pedersen, and Daisuke Shiraki

*Applied Physics and Applied Mathematics, Columbia University, 200 S. W. Mudd Building - MC 4701, 500 W. 120th Street, New York, New York 10027, USA*

(Received 10 June 2008; accepted 30 July 2008; published online 29 August 2008)

The authors report on the first experimental demonstration of active feedback suppression of rotating external kink modes near the ideal wall limit in a tokamak using Kalman filtering to discriminate the  $n=1$  kink mode from background noise. The Kalman filter contains an internal model that captures the dynamics of a rotating, growing  $n=1$  mode. Suppression of the external kink mode is demonstrated over a broad range of phase angles between the sensed mode and applied control field, and performance is robust at noise levels that render proportional gain feedback ineffective. Suppression of the kink mode is accomplished without excitation of higher frequencies as was observed in previous experiments using lead-lag loop compensation [A. J. Klein *et al.*, *Phys Plasmas* **12**, 040703 (2005)]. © 2008 American Institute of Physics. [DOI: [10.1063/1.2974797](https://doi.org/10.1063/1.2974797)]

The appearance of the low- $n$ , ideal, external kink mode in tokamaks at high pressures places the most stringent limit on the maximum achievable  $\beta$ ; i.e., the ratio of the volume-averaged plasma pressure to the magnetic field pressure.<sup>1</sup> The growth rate of the external kink is on the order of the inverse Alfvénic time scale  $1/\tau_A = v_A/a$ , but a conducting wall at the plasma boundary can interact with the mode. The resulting plasma-wall mode is termed a resistive wall mode (RWM), and its growth rate is proportional to the magnetic flux penetration rate of the wall:  $1/\tau_w = R_w/L_w$ . It is possible to construct a wall such that  $\tau_w \gg \tau_A$ , and several experiments have shown that a nearby conducting wall can provide access to  $\beta$  values above the “no-wall” limit.<sup>2,3</sup> Numerical modeling, theory, and experiments have also shown that the RWM may be stabilized by plasma rotation,<sup>4–6</sup> but the velocities required for rotational stabilization in a tokamak burning plasma experiment such as ITER may not be easily and consistently attainable.<sup>7</sup>

Another attractive path to RWM stabilization is the use of feedback with magnetic coils to oppose the perturbed magnetic flux of the mode. Magnetic feedback stabilization of the RWM has been achieved on the High Beta Tokamak-Extended Pulse (HBT-EP) experiment, first with a “smart shell” scheme in which an array of radial sensor and control coils was used to imitate a perfectly conducting wall,<sup>8</sup> and later using an optimized mode control system that employed digital spatial and temporal filtering to detect and suppress the  $n=1$  mode near the ideal wall limit.<sup>9</sup> Success in stabilizing the RWM has also been realized in the DIII-D and NSTX experiments using similar methods.<sup>10,11</sup> The mode control feedback schemes typically used spatial filtering to detect low- $n$  components of the perturbed magnetic field, discarding  $n=0$  and higher-order harmonics unrelated to the RWM. However, filtering to reduce the deleterious effects of mea-

surement noise and sensor pick-up due to other magnetohydrodynamic (MHD) activity, such as edge-localized modes (ELMs), was absent.

Several model-based mode identification algorithms, most employing a Kalman observer,<sup>12</sup> have been proposed for tokamak RWM feedback and tested numerically.<sup>13–17</sup> The Kalman filter compares the results of an internal model for the dynamics of a system with measurements of some or all of these dynamics, producing an estimate that is optimal if the measurements are tainted by Gaussian noise. All of the algorithms cited use system models that account for the dynamics of the RWM in the presence of control inputs and passive conducting structures in varying levels of detail, and show promise in increasing feedback robustness in the presence of white noise and/or that due to ELMs. The only algorithm that has been tested in a closed-loop scenario with an RWM-unstable plasma is that of In *et al.*,<sup>16</sup> but using the Kalman filter did not suppress the RWM. Additionally, none have system models that account for the possibility of a rotating mode. Mode rotation is an important factor to consider when designing RWM feedback algorithms, because feedback that is out of phase with the mode can easily excite and drive the mode, rather than suppress it.<sup>9</sup> In cases where the rotation rate of the mode is changing on time scales close to the controller latency, the optimal phasing between applied feedback and the unstable mode may be lost.

In this letter, we report on the first use of a Kalman filter in suppressing rotating external kink modes. The filter algorithm relies on spatial and temporal filtering for a measurement of the  $n=1$  mode’s amplitude and phase and uses a system model with only two free parameters: The mode’s growth and rotation rates. Mode control feedback with the Kalman filter remains effective at noise levels that make feedback using only proportional gain ineffective.

The HBT-EP experiment<sup>18,19</sup> incorporates a segmented, close-fitting conducting wall made from 20 alternating stain-

<sup>a)</sup>Electronic mail: [jmh2130@columbia.edu](mailto:jmh2130@columbia.edu).

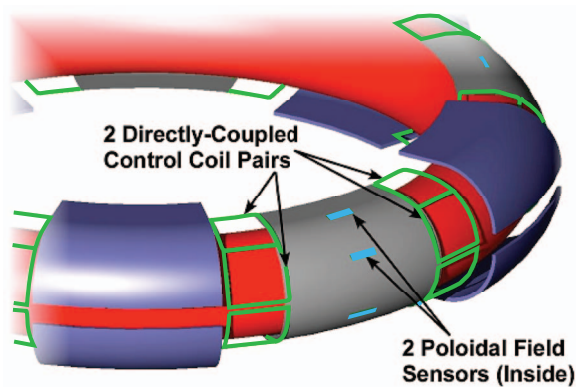


FIG. 1. (Color) The arrangement of the conducting wall sections, radial control coils, and poloidal sensor coils on HBT-EP.

less steel and aluminum sections. Each section may be independently positioned in the minor radial direction between  $r=15$  cm and  $r=23$  cm, providing access to a great range of average wall times. For the experiments described here, the wall was configured for  $\tau_w \approx 500 \mu\text{s}$ .

Feedback control of external MHD activity is accomplished using an array of 20 pairs of radial control coils mounted in the gaps between the wall sections and 20 poloidal sensor coils mounted on the plasma-facing side of the stainless steel wall sections, two per section. Figure 1 shows the three-dimensional arrangement of the wall sections, control coils, and sensor coils. The array of control and sensor coils is divided into four independent feedback loops; each forms a complete toroidal circle at a constant poloidal angle and is driven by a separate field programmable gate array (FPGA) controller. The FPGAs have a sample interval of  $5 \mu\text{s}$  and an overall latency (due to the execution time of the control algorithm) of  $\sim 10 \mu\text{s}$ .

As an alternative to a frequency-dependent amplitude and phase transfer function approach to designing feedback control algorithms, the Kalman filter formulation employs the concept of a system state that evolves in the time domain.<sup>12,20</sup> The system state  $\vec{x}(t)$  and the measurement of that state  $\vec{y}(t)$  evolve according to a linear model of the form

$$\begin{aligned} \frac{d\vec{x}}{dt} &= A\vec{x} + B\vec{u}(t) + \vec{w}(t), \\ \vec{y} &= C\vec{x} + \vec{v}(t). \end{aligned} \quad (1)$$

Here, the matrices  $A$  and  $C$  contain models for the system and measurement dynamics, and  $\vec{w}$  and  $\vec{v}$  represent noise or uncertainties in the system model and the measurements. The matrix  $B$  characterizes the system response to a control input  $\vec{u}$  according to a prescription from Ref. 19. Given the system dynamics matrices, noise covariances, and a set of real-time measurements, the Kalman filter provides an estimate  $\vec{x}^*(t)$  for the state of the system that is optimal if  $\vec{w}$  and  $\vec{v}$  have Gaussian probability distribution functions.

To characterize a growing, rotating instability such as the external kink mode observed in HBT-EP plasmas, the state vector contains the  $n=1$  sine and cosine components of the perturbed poloidal magnetic field. The system model is

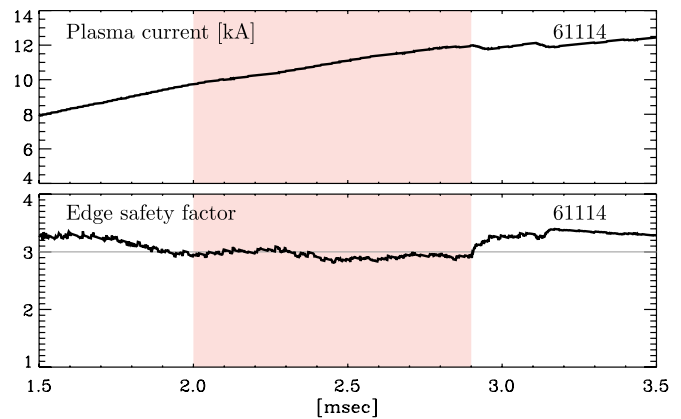


FIG. 2. (Color online) Evolutions of the plasma current and edge safety factor for a typical discharge in the feedback experiments. The external kink mode appears when  $q=3$  surface is near the edge of the plasma, in the range  $2.0 < t < 2.9$  ms.

$$A = \begin{pmatrix} \gamma_0 & -\omega \\ \omega & \gamma_0 \end{pmatrix},$$

with a constant, complex growth rate  $\gamma = \gamma_0 + i\omega$  chosen to match experimental observations. Because the process of making a measurement of the  $n=1$  mode is well addressed by the spatial and temporal filters designed for earlier work,<sup>9</sup> the  $C$  matrix is taken to be the identity transformation, and the Kalman filter is situated between these filters in the control algorithm.

In order to study the efficacy of Kalman filter feedback on external kink modes, current driven kinks were excited in HBT-EP by ramping the plasma current using transformer action. When the current ramp is sufficiently steep, the current density profile becomes very broad with a large edge current density. Under these conditions, rotating external kink modes that are resonant with the outermost  $q$ -surface are observed. The rotation rate of the modes is near 5 kHz, their growth rate is about  $2-3 \text{ ms}^{-1}$ , and they are believed to be near the ideal wall stability limit.<sup>9,18</sup> Figure 2 shows the evolution of the plasma current and edge safety factor  $q_a$  for one of the discharges studied. Magnetic fluctuations with an  $m=3, n=1$  helicity are observed when  $q_a \approx 3$ .

Feedback with the Kalman filter algorithm was observed to both suppress and excite the magnetic fluctuations of the mode according to the spatial phasing of the applied field relative to that of the mode  $\Delta\Phi_f$  (see Fig. 3). To produce the phase-frequency plot in Fig. 4, the feedback phase angle was scanned in  $10^\circ$  increments, and three discharges were made for each setting. Fluctuations measured by a poloidal sensor coil were then Fourier analyzed and averaged together by phase angle. The results show clear regions of excitation and suppression in the 5 kHz band, separated in  $\Delta\Phi_f$ -space by  $180^\circ$ . No significant excitation of frequencies above 8 kHz was observed at any setting of the feedback phase angle.

In order to demonstrate the Kalman filter's ability to produce reliable estimates of the mode's amplitude and phase with noisy inputs, additional noise was mixed with the sensor coil measurements in the feedback algorithm. The noise had an approximately Gaussian probability distribution

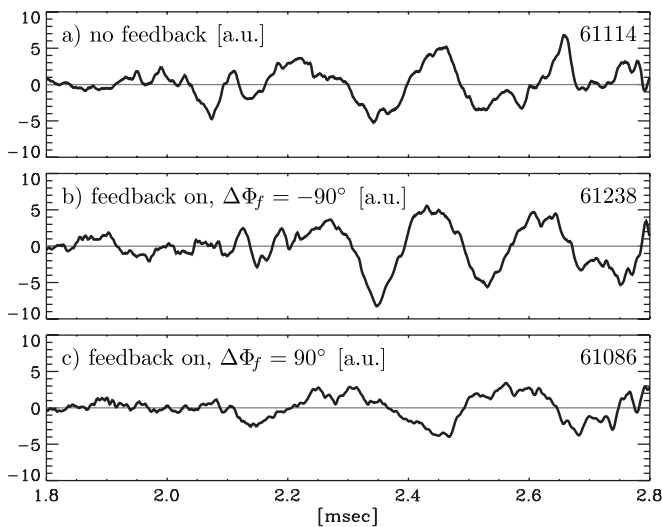


FIG. 3. Poloidal field fluctuations measured 1 cm from the plasma surface for (a) no feedback, (b) positive feedback using the Kalman filter, and (c) negative feedback with the Kalman filter.

with zero mean and a flat frequency spectrum. It was introduced after the Discrete Fourier Transform (DFT) stage in the algorithm, effectively adding a random amplitude and phase to the measured  $n=1$  mode. The amplitude of the added noise was chosen so that its RMS level was close to that of the signals from the sensor coils. Figure 5 shows a calculation of the cosine component of the  $n=1$  mode with the added noise and example output from the feedback algorithm with and without the Kalman filter. When the Kalman filter is absent from the feedback algorithm, the spatial and temporal filters remain; this case is referred to as “ $n=1$  mode ID.” Figure 6 shows the shot-averaged frequency response in the sensor coils for the Kalman filter and  $n=1$  mode ID algorithms with and without any added noise. Without any

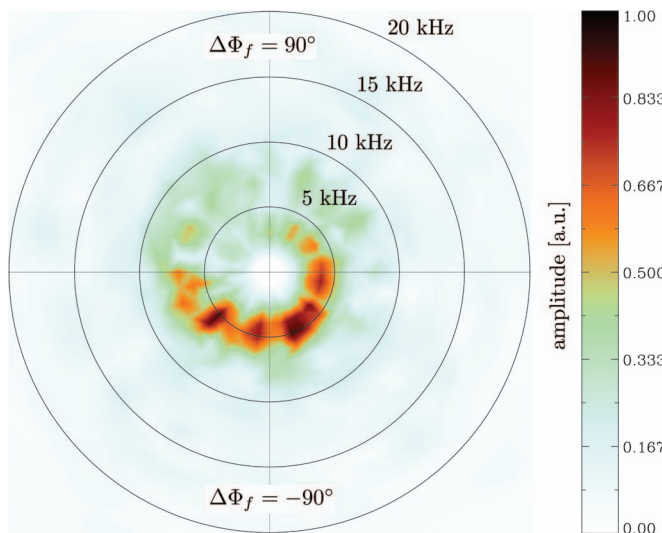


FIG. 4. (Color) Frequency spectrum of poloidal field fluctuations in arbitrary units as a function of the phase angle between feedback and the measured  $n=1$  mode. Feedback may be phased to either suppress or excite the mode near 5 kHz, but the Kalman filter prevents excitation at higher frequencies.

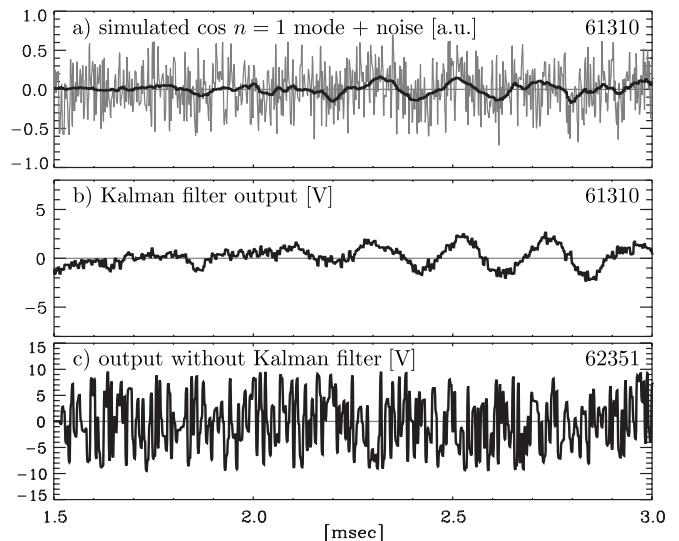


FIG. 5. Adding flat-spectrum, Gaussian noise to the  $n=1$  mode calculated by the FPGA algorithm showcases the Kalman filter’s noise removal capability. Plot (a) shows a simulation of the  $n=1$  cosine mode as calculated in the DFT step in the algorithm (black) and the sum of this signal with the cosine component of the added noise (gray). Plots (b) and (c) show one of five FPGA outputs to the control coils in the added noise experiments for algorithms with and without the Kalman filter, phased to excite the mode.

extra noise, the performance of both filters in exciting and suppressing fluctuations near 5 kHz is comparable. When the noise is added, however, the Kalman filter algorithm retains its ability to excite and suppress the mode, while the  $n=1$  mode ID algorithm does not.

In summary, suppression and excitation of the external kink mode using a Kalman filter has been demonstrated. The Kalman filter estimates the amplitude and phase of an  $n=1$  instability using a simple model of a growing, rotating mode.

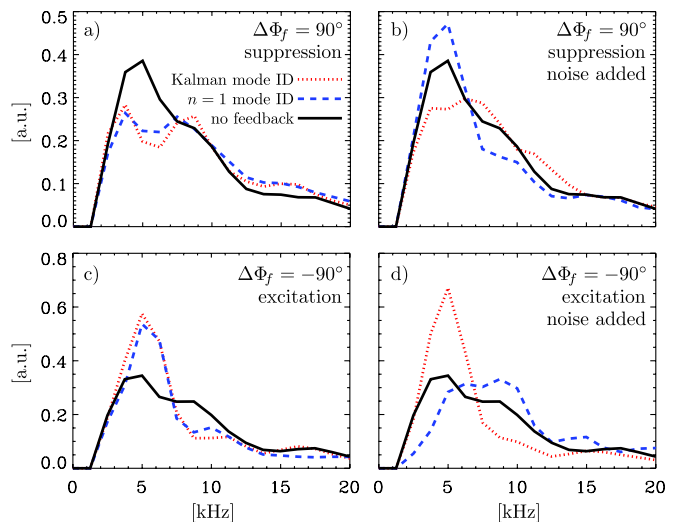


FIG. 6. (Color online) A comparison of the frequency spectrum of the poloidal field for added noise experiments, for feedback off (solid), Kalman filter mode ID feedback (dotted), and  $n=1$  mode ID feedback (dashed) discharges. Plots (a) and (c) show suppression and excitation experiments with no added noise. Plots (b) and (d) show the suppression and excitation cases with extra noise added to the feedback algorithms. With the added noise, the algorithm without the Kalman filter loses its ability to suppress and excite the mode, while the Kalman filter algorithm does not.

Using the Kalman filter prevents excitation at frequencies higher than that of the unstable mode, and the ability of the Kalman filter algorithm to suppress and excite the mode is not affected by presence of noise at amplitudes that disrupt proportional gain only feedback.

The authors gratefully acknowledge the technical support of N. Rivera and J. Andrello during the course of this work.

This work was supported by the U.S. Department of Energy Grant No. DE-FG02-86ER53222.

<sup>1</sup>E. J. Strait, *Phys. Plasmas* **1**, 1415 (1994).

<sup>2</sup>T. S. Taylor, E. J. Strait, L. L. Lao, M. Mauel, A. D. Turnbull, K. H. Burrell, M. S. Chu, J. R. Ferron, R. J. Groebner, R. J. La Haye, B. W. Rice, R. T. Snider, S. J. Thompson, D. Wrblewski, and D. J. Lightly, *Phys. Plasmas* **2**, 2390 (1995).

<sup>3</sup>T. H. Ivers, E. Eisner, A. Garofalo, R. Kombargi, M. E. Mauel, D. Maurer, D. Nadle, G. A. Navratil, M. K. V. Sankar, M. Su, E. Taylor, Q. Xiao, R. R. Bartsch, W. A. Reass, and G. A. Wurden, *Phys. Plasmas* **3**, 1926 (1996).

<sup>4</sup>A. Bondeson and D. J. Ward, *Phys. Rev. Lett.* **72**, 2709 (1994).

<sup>5</sup>R. Betti and J. P. Freidberg, *Phys. Rev. Lett.* **74**, 2949 (1995).

<sup>6</sup>A. M. Garofalo, E. J. Strait, L. C. Johnson, R. J. La Haye, E. A. Lazarus, G. A. Navratil, M. Okabayashi, J. T. Scoville, T. S. Taylor, and A. D. Turnbull, *Phys. Rev. Lett.* **89**, 235001 (2002).

<sup>7</sup>T. C. Hender, J. C. Wesley, J. Bialek, A. Bondeson, A. H. Boozer, R. J. Buttery, A. Garofalo, T. P. Goodman, R. S. Granetz, Y. Gribov, O. Gruber, M. Gryaznevich, G. Giruzzi, S. Günter, N. Hayashi, P. Helander, C. C. Hegna, D. F. Howell, D. A. Humphreys, G. T. A. Huysmans, A. W. Hyatt, A. Isayama, S. C. Jardin, Y. Kawano, A. Kellman, C. Kessel, H. R. Koslowski, R. J. La Haye, E. Lazzaro, Y. Q. Liu, V. Lukash, J. Manickam, S. Medvedev, V. Mertens, S. V. Mirnov, Y. Nakamura, G. Navratil, M. Okabayashi, T. Ozeki, R. Paccagnella, G. Pautasso, F. Porcelli, V. D. Pustovitov, V. Riccardo, M. Sato, O. Sauter, M. J. Schaffer, M. Shimada, P. Sonato, E. J. Strait, M. Sugihara, M. Takechi, A. D. Turnbull, E.

Westerhof, D. G. Whyte, R. Yoshino, H. Zohm, and the ITPA MHD Disruption and Magnetic Control Topical Group, *Nucl. Fusion* **47**, S128 (2007).

<sup>8</sup>C. Cates, M. Shilov, M. E. Mauel, G. A. Navratil, D. Maurer, S. Mukherjee, D. Nadle, J. Bialek, and A. Boozer, *Phys. Plasmas* **7**, 3133 (2000).

<sup>9</sup>A. J. Klein, D. A. Maurer, T. S. Pedersen, M. E. Mauel, G. A. Navratil, C. Cates, M. Shilov, Y. Liu, N. Stillits, and J. Bialek, *Phys. Plasmas* **12**, 040703 (2005).

<sup>10</sup>A. M. Garofalo, E. J. Strait, J. M. Bialek, E. D. Fredrickson, M. Gryaznevich, T. H. Jensen, L. C. Johnson, R. J. La Haye, G. A. Navratil, E. A. Lazarus, T. C. Luce, M. Makowski, M. Okabayashi, B. W. Rice, J. T. Scoville, A. D. Turnbull, M. L. Walker, and the DIII-D Team, *Nucl. Fusion* **40**, 1491 (2000).

<sup>11</sup>S. A. Sabbagh, R. E. Bell, J. E. Menard, D. A. Gates, A. C. Sontag, J. M. Bialek, B. P. LeBlanc, F. M. Levinton, K. Tritz, and H. Yuh, *Phys. Rev. Lett.* **97**, 045004 (2006).

<sup>12</sup>R. E. Kalman, *J. Basic Eng.* **82**, 35 (1960).

<sup>13</sup>C. M. Fransson, D. H. Edgell, D. A. Humphreys, and M. L. Walker, *Phys. Plasmas* **10**, 3961 (2003).

<sup>14</sup>A. K. Sen, M. Nagashima, and R. W. Longman, *Phys. Plasmas* **10**, 4350 (2003).

<sup>15</sup>Z. Sun, A. K. Sen, and R. W. Longman, *Phys. Plasmas* **13**, 012512 (2006).

<sup>16</sup>Y. In, J. S. Kim, D. H. Edgell, E. J. Strait, D. A. Humphreys, M. L. Walker, G. L. Jackson, M. S. Chu, R. Johnson, R. J. La Haye, M. Okabayashi, A. M. Garofalo, and H. Reimerdes, *Phys. Plasmas* **13**, 062512 (2006).

<sup>17</sup>O. Katsuro-Hopkins, J. Bialek, D. Maurer, and G. Navratil, *Nucl. Fusion* **47**, 1157 (2007).

<sup>18</sup>M. Shilov, C. Cates, R. James, A. Klein, O. Katsuro-Hopkins, Y. Liu, M. E. Mauel, D. A. Maurer, G. A. Navratil, T. S. Pedersen, N. Stillits, R. Fitzpatrick, and S. F. Paul, *Phys. Plasmas* **11**, 2573 (2004).

<sup>19</sup>M. E. Mauel, J. Bialek, A. H. Boozer, C. Cates, R. James, O. Katsuro-Hopkins, A. Klein, Y. Liu, D. A. Maurer, D. Maslovsky, G. A. Navratil, T. S. Pedersen, M. Shilov, and N. Stillits, *Nucl. Fusion* **45**, 285 (2005).

<sup>20</sup>R. G. Brown and P. Y. C. Hwang, *Introduction to Random Signals and Applied Kalman Filtering*, 3rd ed. (John Wiley & Sons, New York, 1997).